tvst

DOI: 10.1167/tvst.2.2.4

Article

Rhodopsin F45L Allele Does Not Cause Autosomal Dominant Retinitis Pigmentosa in a Large Caucasian Family

Andrea L. Vincent[1,2,*], Joseph Carroll[3,4,*], Gerald A. Fishman[5], Alexandra Sauer[6], Dianne Sharp[2], Phyllis Summerfelt[3], Vesper Williams[3], Adam M. Dubis[4], Susanne Kohl[6], and Fulton Wong[7,8]

[1] Department of Ophthalmology, New Zealand National Eye Centre, University of Auckland, Auckland, New Zealand
[2] Eye Department, Greenlane Clinical Centre, Auckland District Health Board, Auckland, New Zealand
[3] Department of Ophthalmology, Medical College of Wisconsin, Milwaukee, WI
[4] Department of Cell Biology, Neurobiology and Anatomy, Medical College of Wisconsin, Milwaukee, WI
[5] Pangere Center for the Study of Inherited Retinal Disease, Chicago Lighthouse for People Who Are Blind or Visually Impaired, Chicago, IL
[6] Molecular Genetics Laboratory, Institute for Ophthalmic Research, Centre for Ophthalmology, University Tübingen, Tübingen, Germany
[7] Department of Ophthalmology, Duke University School of Medicine, Durham, NC
[8] Department of Neurobiology, Duke University School of Medicine, Durham, NC

Correspondence: Fulton Wong, Departments of Ophthalmology & Neurobiology, Duke University School of Medicine, Durham, NC, USA. e-mail: fulton.wong@duke.edu.

Received: 9 November 2012
Accepted: 24 January 2013
Published: 14 March 2013

Keywords: exome sequencing; adaptive optics; rhodopsin mutations; retinitis pigmentosa; retinal degeneration

Citation: Vincent AL, Carroll J, Fishman GA, et al. *Rhodopsin* F45L allele does not cause autosomal dominant retinitis pigmentosa in a large caucasian family. Trans Vis Sci Tech. 2013;2(2):4, http://tvstjournal.org/doi/full/10.1167/tvst.2.2.4, doi:10.1167/tvst.2.2.4

Purpose: To ascertain the potential pathogenicity of a retinitis pigmentosa (RP)-causing *RHO* F45L allele in a family affected by congenital achromatopsia (ACHM).

Methods: Case series/observational study that included two patients with ACHM and 24 extended family members. Molecular genetic analysis was performed to identify *RHO* F45L carrier status in the family and a control population. An adaptive optics scanning light ophthalmoscope (AOSLO) was used to image the photoreceptor mosaic and assess rod and cone structure. Spectral domain optical coherence tomography (SD-OCT) was used to examine retinal lamination. Comprehensive clinical testing included acuity, color vision, and dilated fundus examination. Electroretinography was used to assess rod and cone function.

Results: Five carriers of the *RHO* F45L allele alone (24–80 years) and three carriers in combination with a heterozygous *CNGA3* mutant allele (10–64 years) were all free of the classic symptoms and signs of RP. In heterozygous carriers of both mutations, SD-OCT showed normal retinal thickness and intact outer retinal layers; rod and cone densities were within normal limits on AOSLO. The phenotype in two individuals affected with ACHM and harboring the *RHO* F45L allele was indistinguishable from that previously reported for ACHM.

Conclusions: The *RHO* F45L allele is not pathogenic in this large family; hence, the two ACHM patients would unlikely develop RP in the future.

Translational Relevance: The combined approach of comprehensive molecular analysis of individual genomes and noninvasive cellular resolution retinal imaging enhances the current repertoire of clinical diagnostic tools, giving a substantial impetus to personalized medicine.

Introduction

Comprehensive sequencing of the entire genome or exome of individual persons at affordable cost and widely accessible databases of annotated human genomic sequences have given impetus to personalized genomic medicine.[1–3] Since new DNA sequencing technology enables the examination of all genes of a single person simultaneously, occasionally rare and unsuspected alleles associated with specific diseases may be uncovered along with mutations in genes that are anticipated according to the known clinical phenotype.[4] Here, we report on an event in which the initial exome sequencing data predicted dire consequences for two siblings diagnosed with achromatopsia (ACHM).[5] Patients with this hereditary

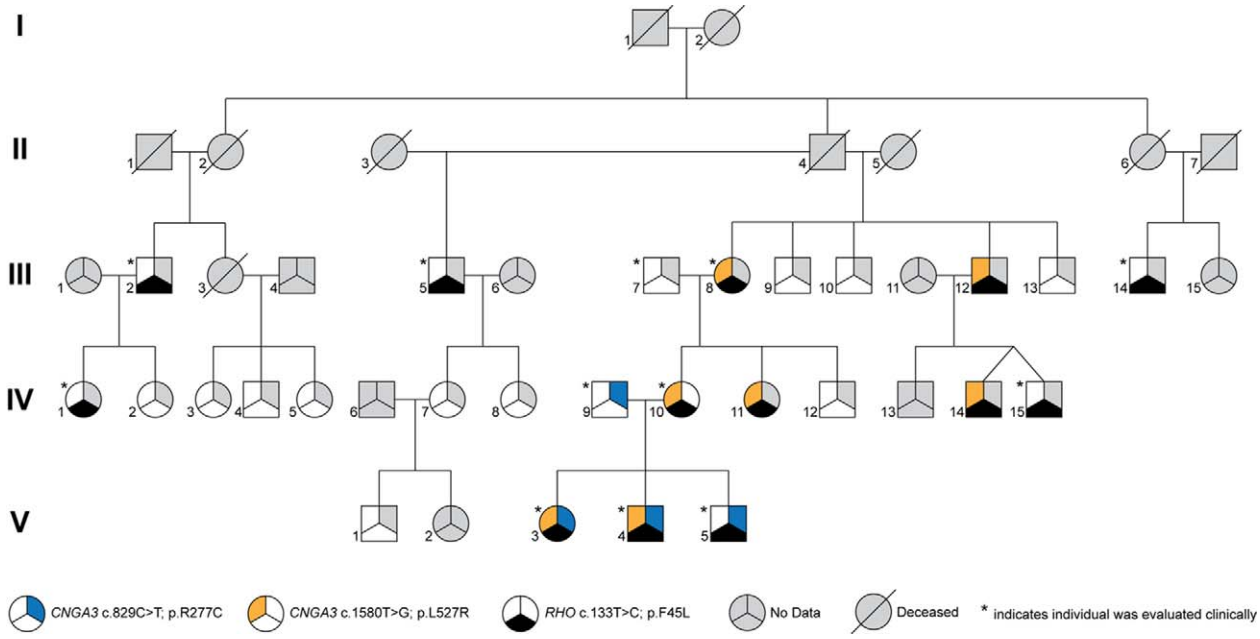

Figure 1. Pedigree of a family harboring two compound heterozygous *CNGA3* mutations (R277C and L527R) and a *RHO* F45L mutation. The three segments within each symbol represent the three alleles, with an open segment reflecting wild type. *Light gray* indicates no data for that allele; an individual with all three segments in *gray* would indicate no genetic data were obtained for that person. V:3 and V:4 presented clinically with ACHM caused by compound heterozygous *CNGA3* mutations, which they inherited from their mother (L527R) and their father (R277C).

condition have virtually no cone photoreceptor function (rod monochromacy) beginning in early childhood; the residual rod-mediated function is the mainstay of their vision. When the clinical diagnosis was confirmed by the identification of mutations in a gene that is critical for cone phototransduction (*CNGA3*) using whole exome sequencing, the process simultaneously revealed that they also harbor a mutant *RHO* allele (F45L), which has been reported to cause autosomal dominant retinitis pigmentosa (RP).[6–9] The possibility that these children could develop additional severe visual loss in adulthood due to loss of both cone and rod functions prompted us to investigate further the pathogenicity of the *RHO* F45L allele,[6–9] and to assess directly the structural integrity of the subjects' photoreceptors by the newly available noninvasive live imaging of rods and cones.[10–12]

The prevalence of ACHM is estimated to be 1 in 30,000 worldwide.[13] To date, mutations in five genes are known to associate with ACHM; these genes encode essential components of cone phototransduction.[14–22] Therefore, the biological disease mechanism of ACHM is a defective phototransduction cascade in all three types of cones. Two pathogenic ACHM-causing mutations in the two siblings were identified initially by exome sequencing (proband, individual V:3 in Fig. 1); they are two compound heterozygous mutations c.829C>T p.R277C and c.1580T>G p.L527R[5] in the *CNGA3* gene that encodes the channel-forming α-subunit of the cone-specific cyclic nucleotide (cGMP)-gated cation channel.[18] These mutations are pathogenic and, thus, they confirmed the clinical diagnosis.

The group of hereditary rod–cone dystrophies collectively known as RP affects approximately 1 in 4000 persons worldwide.[23] Genetically and clinically, RP is notably heterogeneous. Nearly 50 genes are known to be associated with the different genetic types of RP, and there are over 100 mutations identified in the gene encoding rhodopsin, the visual pigment that initiates the phototransduction cascade in rod photoreceptors (http://www.sph.uth.tmc.edu/retnet). The clinical phenotypes, including severity and age of onset, caused by mutations in *RHO* vary widely: from severe, retina-wide impaired rod function early in life to mildly compromised vision (20/25) that can be compatible with normal rods in late adult life.[24–26] While there is clearly allelic specificity, which may correlate with the multiple underlying pathogenic mechanisms, including defective phototransduction and failure of rhodopsin targeting to the photorecep-

tor outer segment,[9] environmental and epigenetic factors most likely contribute to individual and intrafamilial variations of disease severity as well.[9, 24, 25] In other words, while projections of genotype–phenotype correlations can be made statistically in groups,[6] the detailed phenotypic expression of a particular *RHO* mutation in a person is far from predictable.[9, 24, 25] The mutant *RHO* F45L allele was first reported in 1 of 161 unrelated patients with autosomal dominant RP and not in 118 normal subjects; it cosegregated in eight (five affected, three unaffected) members of a three generation family.[9] Another family affected by the *RHO* F45L allele was characterized and reported by Berson et al.[6] Amino acid F45 is 100% conserved among vertebrate rhodopsins, indicating that it may serve an important biological function.[27] Commonly used prediction software of protein function such as PolyPhen2 (http://genetics.bwh.harvard.edu/pph2/) calls *RHO* F45L as 'probably damaging'; SIFT analysis (http://sift.jcvi.org/) classifies this change 'deleterious'. While *RHO* F45L might not alter protein stability,[9, 28] analysis using a structure-based approach has suggested that its location at the dimer interface possibly impacts dimer formation/stability and, thus, could affect rod phototransduction.[29–31] Because of the very few unrelated RP patients reported with the *RHO* F45L allele,[6–9] we sought to identify additional carriers to ascertain the phenotype.

Methods

This study adhered to the tenets of the Declaration of Helsinki and had institutional ethics approval from the University of Auckland (NTX 08-12-123/A+4290), Medical College of Wisconsin (CHW 07/77), Chicago Lighthouse for People Who Are Blind or Visually Impaired, and the University of Tübingen. Members of the nuclear family and extended family of the proband's maternal grandmother (individual III:8 in Fig. 1) were identified and recruited following informed consent. Normal controls unrelated to the family and autosomal dominant RP patients were included as well.

Blood/DNA samples of patients and healthy subjects analyzed retrospectively in this study were recruited and collected over a 20 year period.

Mutation Analysis

Biological samples (peripheral venous blood or saliva) were collected for DNA extraction to screen for *RHO* F45L and/or *CNGA3* L527R alleles. Since this family is of European descent, we screened 597 unrelated normal controls of similar ethnicity and 115 autosomal dominant RP patients for F45L. Family and control DNA samples were screened for *CNGA3* c.1580T>G (Primers forward: 5′-GAGCCTCCCA-GACAAGCTGAAG-3′ and reverse: 5′-AGTAGC-CAATGCTGCGGATGTT-3′.) and *RHO* c.113T>C via polymerase chain reaction (PCR) and direct Sanger sequencing on an ABI 3700 prism genetic analyzer (Applied Biosystems Inc., Foster City, CA). Further details of PCR primers and conditions, purification and sequencing are described in the **Supplemental Information**. Nucleotide sequences were compared with the National Center for Biotechnology Information reference sequences (*CNGA3* NC_000,002.11 and *RHO* NG_009,115.1) using CodonCode Aligner version 3.5.1 (CodonCode Corporation, Centerville, MA).

Clinical Examination

Selected individuals (asterisks, Fig. 1), identified following mutational analysis of *CNGA3* and *RHO*, underwent comprehensive ophthalmic examination including Snellen visual acuity, color vision testing, slit lamp biomicroscopy, and dilated fundoscopy. Spectral domain optical coherence tomography (SD-OCT) and fundus autofluorescence were acquired using Spectralis HRA + OCT (Heidelberg Engineering, Heidelberg, Germany), and standard electrodiagnostic assessment (pattern and flash electroretinograms) was recorded according to the International Society for Clinical Electrophysiology of Vision (ISCEV) standards using gold foil electrodes and full field Ganzfeld stimulus with Roland-Consult equipment.

Adaptive Optics Imaging of the Photoreceptor Mosaic

To examine the subclinical structure of the rods and cones in the three children of the nuclear family, two affected (V:3, V:4) and the unaffected sibling V:5 (carrier of both F45L and R277C), as well as their mother (IV:10) and grandmother (III:8), who are carriers of both F45L and L527R, were assessed using an adaptive optics scanning light ophthalmoscope (AOSLO), performed in the Department of Ophthalmology at the Medical College of Wisconsin in Milwaukee, Wisconsin. For individuals undergoing AOSLO imaging, further high density SD-OCT line scans through the fovea were obtained, with a sampling of 1000 A-scans/B-scan and 100 repeated

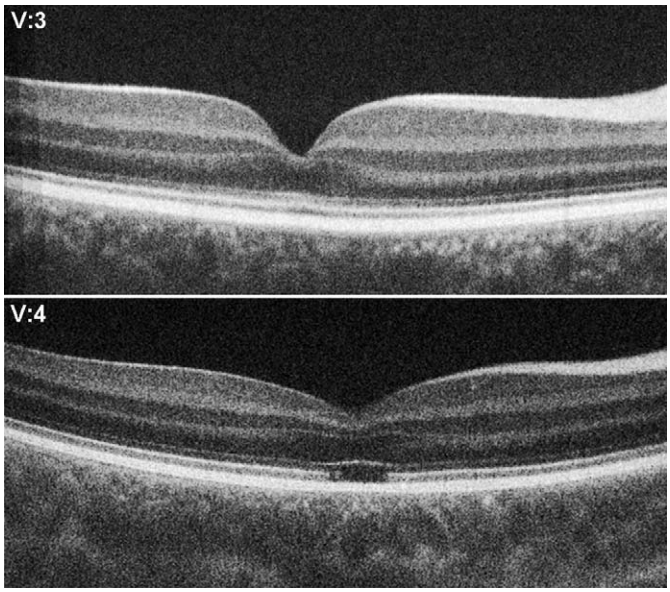

Figure 2. High resolution SD-OCT scans through the fovea in ACHM patients. Shown are images from two siblings (V:3 and V:4) diagnosed with ACHM. Despite differences in the appearance of the outer retinal layers, the findings are consistent with previous reports in ACHM.[12, 40]

B-scans (Bioptigen, Inc., Durham, North Carolina). Up to 40 B-scans from these 100-scan sequences were registered and averaged to reduce speckle noise in the image as previously described.[32]

Images of the photoreceptor mosaic were obtained using a previously described AOSLO.[10] The wavelength of the super luminescent diode used for retinal imaging was 775 nm, subtending a field of view of $0.96° \times 0.96°$. Separate image sequences of 100 to 200 frames each were acquired at various parafoveal and perifoveal locations. Parafoveal images were acquired by instructing the patient to fixate on one of the corners of the raster scan square, while the perifoveal images were acquired using an internal fixation target.

Images were processed as previously described, by first correcting for the intraframe distortions within the raw image sequence caused by the sinusoidal motion of the resonant optical scanner.[10] The corrected images were then registered and averaged using a previously described strip-registration algorithm.[33] From these images, cell density was calculated over a 55×55 μm sampling window using a previously described semi-automated algorithm implemented in Matlab (Mathworks, Natick, Massachusetts).[34] Since the rods greatly outnumber the cones in the perifoveal images, we utilized the algorithm to identify the rods by removing any cones during the user review step. Estimates of cone density for these perifoveal images were obtained using manual identification of the large, coarsely spaced cones.

Results

Mutation Analysis and Pedigree

The *RHO* F45L allele was not seen in the 597 unrelated normal controls of European origin, or in 115 autosomal dominant RP patients. Retrospective data analysis showed that this variant had not been seen in an additional 150 independent autosomal dominant RP patients screened earlier. Furthermore, *RHO* F45L is not listed in exome sequencing data from approximately 13,000 alleles (Exome Variant Server, NHLBI Exome Sequencing Project (ESP), Seattle, WA; http://evs.gs.washington.edu/EVS/) nor observed in 1000 Genomes (http://www.1000genomes.org/). These results add to the supporting evidence for the pathogenicity of *RHO* F45L.

Starting with knowledge of the nuclear family, we contacted members of the extended family to construct a pedigree. Early results from individuals III:8 and III:5 (half-brother of III:8) in Figure 1 suggested that the *RHO* F45L allele was inherited from their father. Accordingly, the search was focused on the descendants of his siblings. Individuals were tested for their *CNGA3* L527R and *RHO* F45L carrier status and the results are shown in Figure 1. Our efforts yielded the identification of five members of the extended family who are carriers of the *RHO* F45L allele alone, and five additional individuals with the *RHO* F45L variant also carried a *CNGA3* L527R mutation heterozygously.

Clinical Findings in Patients with ACHM and Who Are Carriers of *RHO* F45L

As reported previously,[5] two individuals in this family (V:3 and V:4) were diagnosed as having ACHM in addition to harboring the *RHO* F45L allele. Detailed clinical examination at age 15 (V:3) and age 12 (V:4) showed a blunted foveal reflex, normal appearance of the optic nerve, normal vessels, and no sign of peripheral degeneration. In both individuals, electroretinogram (ERG) testing using the ISCEV protocol showed nondetectable cone function, both with the single flash and 30-Hz flicker. The isolated rod response was of normal amplitude and implicit time in both individuals, and the maximum combined dark-adapted response was

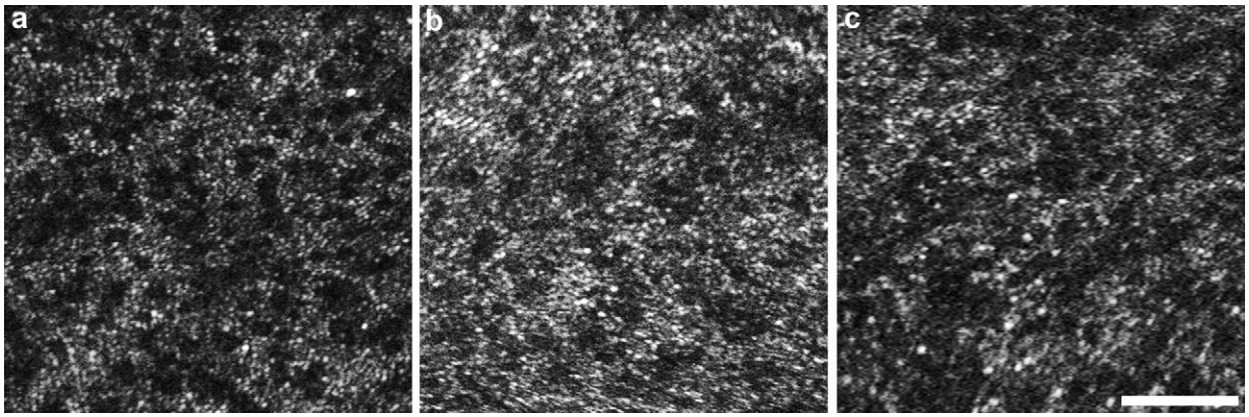

Figure 3. Parafoveal photoreceptor structure in patients with ACHM and *RHO* F45L. Shown are AOSLO images of the photoreceptor mosaic from (a) Subject 8 from Genead et al.,[12] (b) V:3, and (c) V.4. The cone mosaic is disrupted compared with normal, but qualitatively, the two patients with ACHM look similar to those reported previously. Scale bar = 50 μm.

normal in V:4 and just below the normal limit for V:3 (with both having normal implicit time). The ERG data indicate that the patients' rod function was not reduced by the *RHO* F45L allele. These results are consistent with a typical ACHM phenotype and inconsistent with a diagnosis of RP. To see if the presence of the *RHO* F45L allele in any way affected the retinal phenotype, we acquired high resolution retinal images for comparison with previously reported ACHM patients.

As shown in Figure 2 on OCT, V:4 showed foveal cavitation, which has been reported previously in ACHM.[12, 22] While his sister (V:3) did not show this defect, the second hyperreflective band (corresponding to the ellipsoid portion of the inner segment [ISe]) appeared less distinct at the fovea than the periphery. The brother (V:4) also showed incomplete excavation of the inner retinal layers (foveal hypoplasia), while his sister (V:3) did not. Both OCT scans were confirmed to pass through the presumed foveal center by referring to the volume images and identifying the location with the deepest foveal pit and/or most complete excavation of the inner retinal layers. Interestingly, the nystagmus in V:3 was much worse than that for V:4.

Imaging of the photoreceptor mosaic was undertaken with AOSLO. As shown in Figure 3, we observed a significantly disrupted parafoveal photoreceptor mosaic in both of the patients with ACHM, similar to images previously published for other patients with ACHM.[12] In these images, it is thought that the small bright reflective cells are healthy rod photoreceptors, while the larger dark circles represent nonwaveguiding cone photoreceptors. Images of the perifoveal mosaic (Fig. 4) also revealed findings consistent with previous reports in patients with

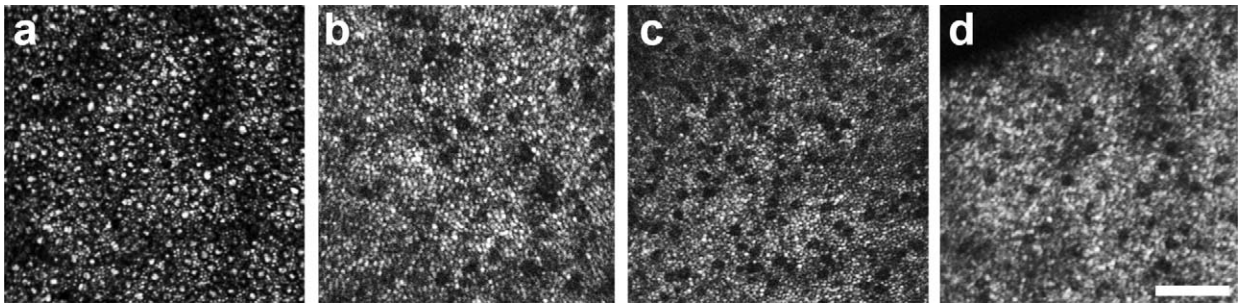

Figure 4. Perifoveal photoreceptor structure in patients with ACHM and *RHO* F45L. Shown are AOSLO images of the photoreceptor mosaic from (a) a normal control, (b) Subject 8, ACHM *CNGB3* homozygote from Genead et al.,[12] and (c) Subject 12 ACHM *CNGA3* heterozygote from Genead et al.[12] (d) V:4 Rod density is 83,300 rods/mm^2, consistent with that reported previously in this location.[11, 35] His cone density (2400 cones/mm^2) is significantly reduced from that expected from these previous studies (~11,000 cones/mm^2). Some nonwaveguiding cones are present, as has been shown in other patients with ACHM.[12] Scale bar = 50 μm. Parts (b) and (c) reproduced with permission from Genead MA, Fishman GA, Rha J, et al. Photoreceptor structure and function in patients with ACHM. Invest Ophthalmol Vis Sci 2011;52:7298-7308.

Table 1. Clinical Characteristics of Individuals Carrying the Rhodopsin Mutation in Isolation

Individual	Sex	Age	*RHO*	*CNGA3*	BCVA		Ishihara		Fundus	OCT	FAF	Other
					RE	LE	RE	LE				
III:2	M	80	F45L+/wt	wt/wt	20/32	20/25	14	15	√	√	√	Mild NS cataract, peripheral lattice degeneration
III:5	M	75	F45L+/wt	wt/wt	20/20	20/20	1/15	1/15	√	√	√	Congenital X-linked colour blindness AMD drusen ERG normal
III:14	M	65	F45L+/wt	wt/wt	20/16	20/12.5	15	15	√	√	√	N/A
IV:1	F	52	F45L+/wt	wt/wt	20/16	20/16	15	15	√	√	√	N/A
IV:15	M	24	F45L+/wt	wt/wt	20/16	20/16	15	15	√	√	√	N/A

M = male, F = female, BCVA = best corrected visual acuity (measured with Snellen chart), RE = Right eye, LE = Left eye, FAF = fundus autofluoresence, NS = nuclear sclerosis, AMD = age-related macular degeneration, N/A = not applicable.

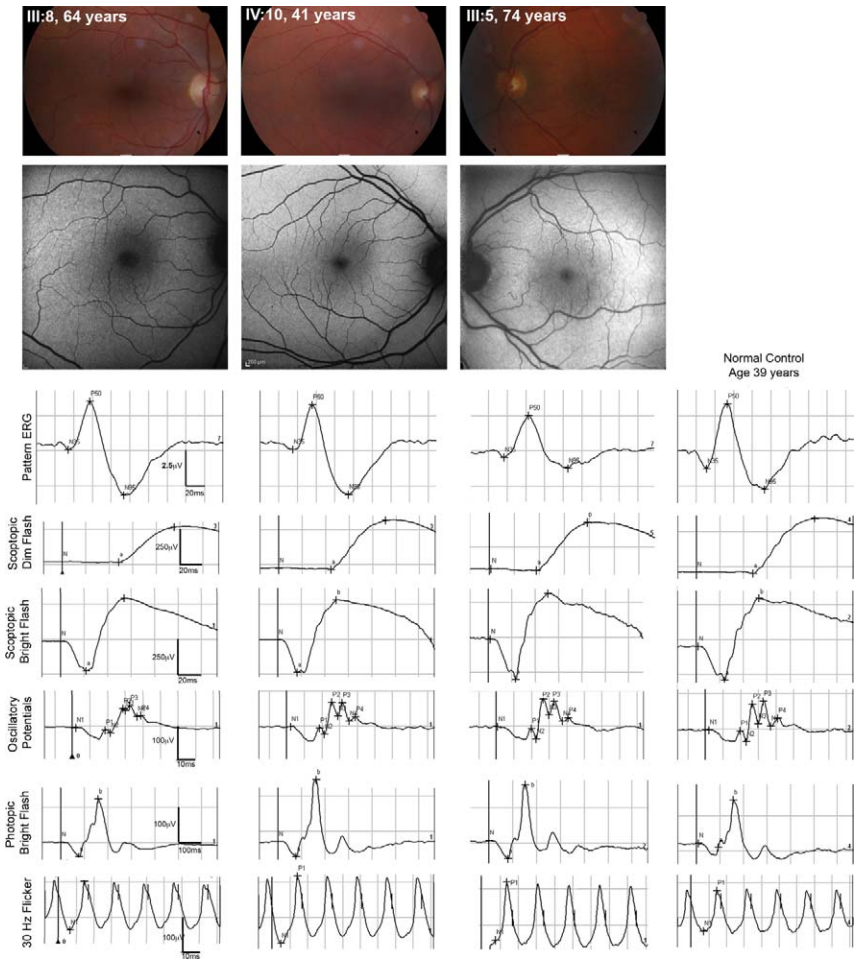

Figure 5. Clinical presentation of *RHO* F45L carriers. Shown are fundus photos (*top*), fundus autofluorescence (*middle*), and electrophysiology results (*bottom*) for III:8, IV:10, and III:5. Individuals III:8 and IV:10 had normal fundus appearance, while III:5 had drusen at the posterior pole, which is not unexpected for a 74-year-old. All displayed normal waveforms to ISCEV standard flash testing, and pattern electroretinogram (pERG). The pERG in III:5 is slightly reduced in amplitude but still within normal limits, with N95:P50 ratio greater than 1.1 in both eyes (right eye 1.25, the eye shown) and left eye 1.46.

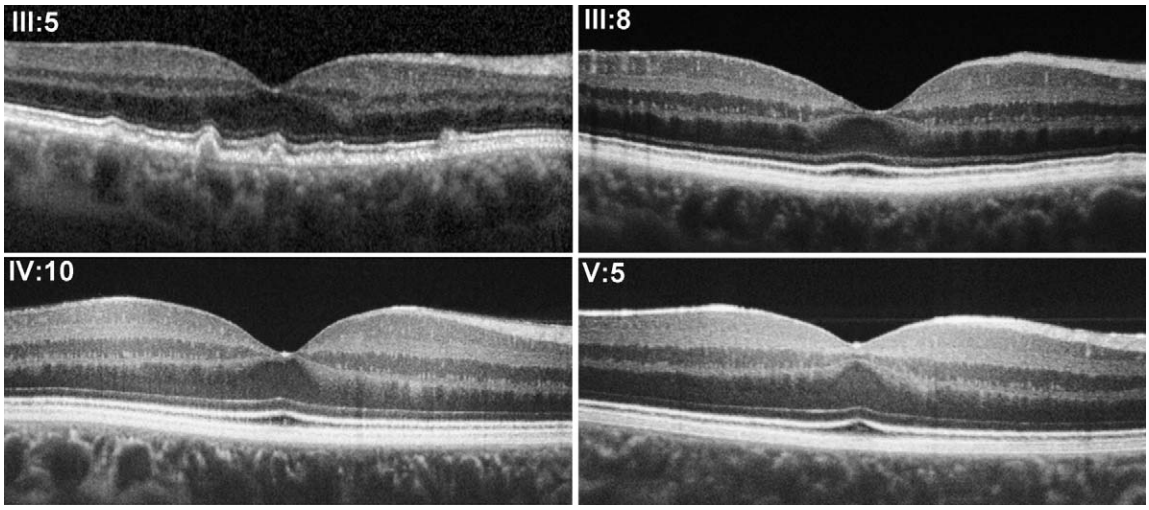

Figure 6. Gross retinal structure in carriers. Shown are SD-OCT images acquired with the Spectralis (III:5) or Bioptigen (III:8, IV:10, V:5). All carriers showed normal retinal lamination, though III:5 had drusen in his macula.

ACHM.[12] Rod density in V:4 was consistent (83,300 rods/mm^2) with that reported previously for this location both in vivo[11] and ex vivo,[35] and as with other rod monochromats, we observed a small population of residual cones, with a density of 2400 cones/mm^2 (Fig. 4D). While this is well below that expected for normals (11,000 cones/mm^2), there do appear to be cones surviving despite the presence of *CNGA3* mutations. Nystagmus was too severe in V:3 to determine the imaging location in her retina (and, thus, reliable quantitative analysis); although qualitatively, her images were similar to those of V:4. Taken together, these data reveal a typical ACHM phenotype that appears to be unaffected by the presence of an *RHO* P45L allele.

Clinical Presentation of *RHO* F45L Carriers

Detailed clinical examination and tests of the five carriers of the *RHO* F45L allele alone (age 24–80 years) showed that they were all free of the classic symptoms and signs of RP. The clinical results are summarized in Table 1.

Figure 5 includes the ERG of one of the five carriers of *RHO* F45L (individual III:5). At age 74, his test results were within the range of healthy controls. He had some mild macular degeneration as indicated by the presence of drusen on his fundus photos. Most importantly, his normal dim flash scotopic response at age 74 ruled out RP. Furthermore, the ERG of two individuals (III:8 and IV:10) who are carriers of *RHO* F45L and *CNGA3* L527R heterozygously (Fig. 5) were also normal. While not examined, all the other double heterozygous carriers of *RHO* F45L and *CNGA3* L527R (Fig. 1) reported no night blindness, which is usually the earliest symptom of RP. The data obtained from this large family are inconsistent with a clinical diagnosis of RP in the carriers of the *RHO* F45L allele.

Retinal Structure in *RHO* F45L Carriers

Examination with SD-OCT showed normal retinal lamination in four *RHO* F45L carriers imaged, though V:5 had incomplete excavation of inner retinal layers at the fovea (Fig. 6). One of these carriers (V:5) was previously shown to carry the *CNGA3* R277C mutations heterozygously as well,[5] and III:8 carried the same *CNGA3* L527R mutation heterozygously as her daughter IV:10. As mentioned above, III:5 only carried *RHO* F45L. All of the hyperreflective bands associated with the photoreceptors[36] appeared continuous and of normal contour (though III:5 did have subretinal mounds corresponding to the drusen visible in his fundus image). Retinal thickness was measured from the OCT volume scans in three of these carriers (III:8, IV:10, V:5) and found to be normal (**Supplementary Figure S1**). These data are consistent with normal retinal structure in these patients, despite the presence of the *RHO* F45L allele.

To examine the subclinical photoreceptor phenotype associated with the *RHO* F45L allele, we obtained images of the rod and cone mosaic in two individuals who carried both *RHO* F45L and a *CNGA3* mutation heterozygously (IV:10 and V:5), as well as a family member who only carried a

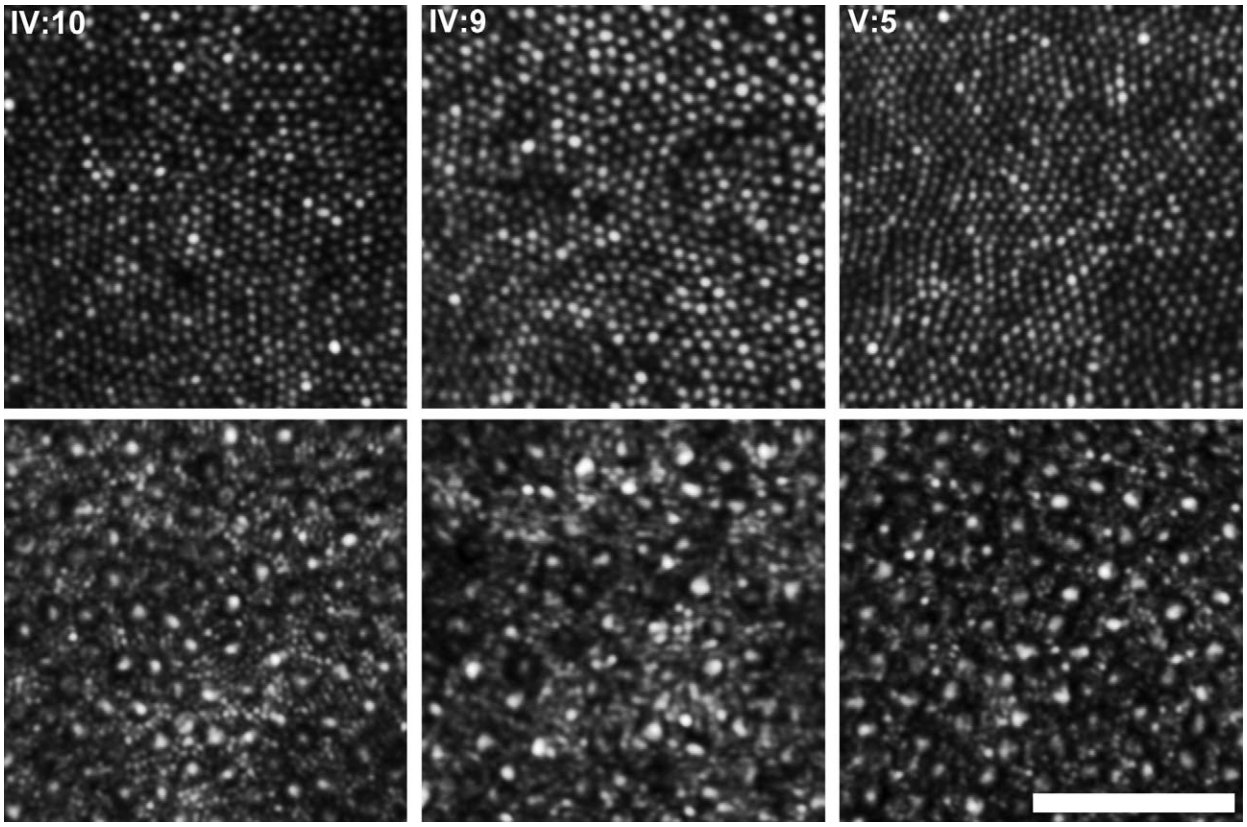

Figure 7. Rod and cone structure in carriers. Images were acquired near the fovea, about 0.6° from fixation (*top row*), and in the periphery, about 10° from fixation (*bottom row*). As shown in Table 2, cone and rod density was not different from normal.

CNGA3 mutation heterozygously (IV:9). Images of the photoreceptor mosaic in these individuals are shown in Figure 7. The images reveal a complete, contiguous cone mosaic near the fovea (top row) and normal rod and cone mosaics at about 10° in the perifovea (bottom row). Cone and rod density for all three were within normal values (Table 2). Collectively, the high resolution imaging tools failed to detect any defect in rod or cone structure in individuals carrying the *RHO* F45L mutation, which is compatible with *RHO* F45L being nonpathogenic.

Discussion

The simplest interpretation of our data is that the *RHO* F45L variant may not be pathogenic. This is consistent with recent work showing the F45L variant to be trafficked normally in neuronal cells and to function as a photolabile pigment with a spectral profile identical to wild type.[37] It can be argued that the true cause of RP in the few previously reported patients is not *RHO* F45L. For the three generation RP family, cosegregation of phenotype in the eight members might be explained by postulating that the actual pathogenic genetic defect is in linkage disequilibrium to *RHO* F45L.[9] The actual mutation may lie in unanalyzed regions of *RHO* (i.e., 5′ or 3′ regulatory sequences or within the introns). Whole exome or genome sequencing of DNA from these RP patients may reveal alternative explanations for their phenotype.

However, accumulated evidence cited in the preceding paragraphs in support of the pathogenicity of *RHO* F45L is fairly strong. Therefore, alternative

Table 2. Cone and Rod Density in Carriers

	Parafovea (0.6°)	Perifovea (10°)	
	Cone Density*	Cone Density*	Rod Density*
IV:10	86,600	10,600	102,100
IV:9	76,700	10,900	86,300
V:5	90,900	9600	93,900

See text for methods used to derive estimates of cell density. All carriers had cone and rod density values within previously published normative values.

*Density values are in cells per square millimeter.

interpretations cannot be dismissed offhand. For example, it is possible that the pathogenicity of F45L is determined by the relative expressivity of the mutant *RHO* allele and the normal *RHO* allele, such that a disease phenotype is absent clinically if the mutant allele has a lower than normal expressivity. This conjectural mechanism is analogous to what underlies incomplete penetrance reported for autosomal dominant RP caused by mutations in *PRPF31*.[38] It is also noted that *PRPF31* encodes a protein essential for pre-mRNA splicing; among the substrates of PRPF31 is rhodopsin. Mutant PRPF31 inhibits pre-mRNA splicing of intron 3 in *RHO*, which results in reduction of *RHO* expression and cell death by apoptosis.[39] Therefore, in addition to its own regulatory mechanisms, *RHO* expression may be modulated by other genes that could determine the relative expressivity of the mutant and normal *RHO* allele.

It is noteworthy, that members of the extended family corroborated on anecdotal reports of visual problems in two deceased potential carriers of *RHO* F45L who were two generations apart. One had noticeable photophobia (individual III:3) and the other "unexplained blindness" around age 30 (sister of I:2). The only three children of the former have normal *RHO* alleles; the latter was not married and had no offspring. Lacking direct information, one could only speculate that these two individuals might have had some symptoms of RP. On that premise, they would likely have harbored the *RHO* F45L allele and chromosomal recombination events could have made the mutant allele more or as expressive as the normal allele, leading to a RP phenotype of variable severity. Even if such spontaneous mutations could in theory occur in V:3 and V:4, the probability is expected to be very small.

From the serendipitous discovery of both cone- and rod-specific mutations in one person to phenotyping individuals with cellular resolution, this study reflects the emerging reality of personalized genomic medicine.[3] As new tools that can provide vast amounts of precise personal genetic information become more available, unique situations that require highly individualized treatment and management such as the case reported here will occur much more often than before the new era of personalized medicine.

Acknowledgments

The authors would like to thank Bryan Hay and Amanda Richards for technical assistance; Brian Higgins, Pooja Godara, Robert Cooper, and Alfredo Dubra for assistance with retinal imaging; and all of the family members for their participation in this study.

*These authors contributed equally to this work.

Financial support. This study was supported by grants from the National Eye Institute (P30EY001931, JC; T32EY014537, AMD; P30EY001792, GAF; and R01EY017607, JC). Additional support from Save Sight Society of New Zealand (AV), Retina NZ (AV), the Ombler Trust (AV), Foundation Fighting Blindness (JC, GAF), Research to Prevent Blindness (JC, FW), The Gene and Ruth Posner Foundation (JC), the RD and Linda Peters Foundation (JC), the Pangere Corporation (GAF), Grant Healthcare Foundation (GAF), and the Thomas M. Aaberg, Sr., Retina Research Fund (JC). This publication was conducted in part in a facility constructed with support from Research Facilities Improvement Program (C06 RR-016511) from the National Center for Research Resources, National Institutes of Health.

Disclosure: **A.L. Vincent**, None; **J. Carroll**, None; **G.A. Fishman**, None; **A. Sauer**, None; **D. Sharp**, None; **P. Summerfelt**, None; **V. Williams**, None; **A.M. Dubis**, None; **S. Kohl**, None; **F. Wong**, None

References

1. Biesecker LG. Exome sequencing makes medical genomics a reality. *Nat Genet*. 2010;42:13–14.
2. Chan IS, Ginsburg GS. Personalized medicine: progress and promise. *Ann Rev Genom Hum Genet*. 2011;12:217–244.
3. Wiggs JL. Genomic promise: personalized medicine for ophthalmology. *Arch Ophthalmol*. 2008; 126:422–423.
4. Ng SB, Buckingham KJ, Lee C, et al. Exome sequencing identifies the cause of a mendelian disorder. *Nat Genet*. 2010;42:30–35.
5. Lam K, Guo H, Wilson GA, Kohl S, Wong F. Identification of variants in CNGA3 as cause for achromatopsia by exome sequencing of a single patient. *Arch Ophthalmol*. 2011;129:1212–1217.
6. Berson EL, Rosner B, Weigel-DiFranco C, Dryja TP, Sandberg MA. Disease progression in patients with dominant retinitis pigmentosa and rhodopsin mutations. *Invest Ophthalmol Vis Sci*. 2002;43:3027–3036.

7. Matias-Florentino M, Ayala-Ramirez R, Graue-Wiechers F, Zenteno JC. Molecular screening of rhodopsin and peripherin/RDS genes in Mexican families with autosomal dominant retinitis pigmentosa. *Curr Eye Res*. 2009;34:1050–1056.
8. Stone EM. Finding and interpreting genetic variations that are important to ophthalmologists. *Trans Am Ophthalmol Soc*. 2003;101:437–484.
9. Sung CH, Davenport CM, Hennessey JC, et al. Rhodopsin mutations in autosomal dominant retinitis pigmentosa. *Proc Natl Acad Sci U S A*. 1991;88:6481–6485.
10. Cooper RF, Dubis AM, Pavaskar A, Rha J, Dubra A, Carroll J. Spatial and temporal variation of rod photoreceptor reflectance in the human retina. *Biomed Opt Express*. 2011;2:2577–2589.
11. Dubra A, Sulai Y, Norris JL, et al. Noninvasive imaging of the human rod photoreceptor mosaic using a confocal adaptive optics scanning ophthalmoscope. *Biomed Opt Express*. 2011;2:1864–1876.
12. Genead MA, Fishman GA, Rha J, et al. Photoreceptor structure and function in patients with congenital achromatopsia. *Invest Ophthalmol Vis Sci*. 2011;52:7298–7308.
13. Sharpe LT, Stockman A, Jagle H, Nathans J. Opsin genes, cone photopigments and colorblindness. In: Gegenfurtner K, Sharpe LT, eds. *Color Vision: from Genes to Perception*. Cambridge: Cambridge University Press; 1999:3–52.
14. Aligianis IA, Forshew T, Johnson S, et al. Mapping of a novel locus for achromatopsia (ACHM4) to 1p and identification of a germline mutation in the alpha subunit of cone transducin (GNAT2). *J Med Genet*. 2002;39:656–660.
15. Chang B, Grau T, Dangel S, et al. A homologous genetic basis of the murine cpfl1 mutant and human achromatopsia linked to mutations in the PDE6C gene. *Proc Natl Acad Sci U S A*. 2009;106:19581–19586.
16. Kohl S, Baumann B, Rosenberg T, et al. Mutations in the cone photoreceptor G-protein alpha-subunit gene GNAT2 in patients with achromatopsia. *Am J Hum Genet*. 2002;71:422–425.
17. Kohl S, Coppieters F, Meire F, et al. A nonsense mutation in PDE6H causes autosomal-recessive incomplete achromatopsia. *Am J Hum Genet*. 2012;91:527–532.
18. Kohl S, Marx T, Giddings I, et al. Total colourblindness is caused by mutations in the gene encoding the alpha-subunit of the cone photoreceptor cGMP-gated cation channel. *Nat Genet*. 1998;19:257–259.
19. Lamb TD, Pugh EN, Jr. Phototransduction, dark adaptation, and rhodopsin regeneration the proctor lecture. *Invest Ophthalmol Vis Sci*. 2006;47:5137–5152.
20. Lerea CL, Bunt-Milam AH, Hurley JB. Alpha transducin is present in blue-, green-, and red-sensitive cone photoreceptors in the human retina. *Neuron*. 1989;3:367–376.
21. Sundin OH, Yang JM, Li Y, et al. Genetic basis of total colourblindness among the Pingelapese islanders. *Nat Genet*. 2000;25:289–293.
22. Thiadens AA, den Hollander AI, Roosing S, et al. Homozygosity mapping reveals PDE6C mutations in patients with early-onset cone photoreceptor disorders. *Am J Hum Genet*. 2009;85:240–247.
23. Dryja TP, Berson EL. Retinitis pigmentosa and allied diseases. Implications of genetic heterogeneity. *Invest Ophthalmol Vis Sci*. 1995;36:1197–1200.
24. Chen H, Chen Y, Horn R, et al. Clinical features of autosomal dominant retinitis pigmentosa associated with a Rhodopsin mutation. *Ann Acad Med Singap*. 2006;35:411–415.
25. Cideciyan AV, Hood DC, Huang Y, et al. Disease sequence from mutant rhodopsin allele to rod and cone photoreceptor degeneration in man. *Proc Natl Acad Sci U S A*. 1998;95:7103–7108.
26. Rodriguez JA, Herrera CA, Birch DG, Daiger SP. A leucine to arginine amino acid substitution at codon 46 of rhodopsin is responsible for a severe form of autosomal dominant retinitis pigmentosa. *Hum Mut*. 1993;2:205–213.
27. Briscoe AD, Gaur C, Kumar S. The spectrum of human rhodopsin disease mutations through the lens of interspecific variation. *Gene*. 2004;332:107–118.
28. Mendes HF, van der Spuy J, Chapple JP, Cheetham ME. Mechanisms of cell death in rhodopsin retinitis pigmentosa: implications for therapy. *Trends Mol Med*. 2005;11:177–185.
29. Jastrzebska B, Goc A, Golczak M, Palczewski K. Phospholipids are needed for the proper formation, stability, and function of the photoactivated rhodopsin-transducin complex. *Biochemistry*. 2009;48:5159–5170.
30. Jastrzebska B, Golczak M, Fotiadis D, Engel A, Palczewski K. Isolation and functional characterization of a stable complex between photoactivated rhodopsin and the G protein, transducin. *FASEB J*. 2009;23:371–381.

31. Rakoczy EP, Kiel C, McKeone R, Stricher F, Serrano L. Analysis of disease-linked rhodopsin mutations based on structure, function, and protein stability calculations. *J Mol Biol*. 2011; 405:584–606.
32. Tanna H, Dubis AM, Ayub N, et al. Retinal imaging using commercial broadband optical coherence tomography. *Br J Ophthalmol*. 2010; 94:372–376.
33. Dubra A, Harvey Z. Registration of 2D images from fast scanning ophthalmic instruments. *Biomedical Image Registration*. Heidelberg, Germany: Springer; 2010:60–71.
34. Garrioch R, Langlo C, Dubis AM, Cooper RF, Dubra A, Carroll J. Repeatability of in vivo parafoveal cone density and spacing measurements. *Optom Vis Sci*. 2012;89:632–643.
35. Curcio CA, Sloan KR, Kalina RE, Hendrickson AE. Human photoreceptor topography. *J Comp Neurol*. 1990;292:497–523.
36. Spaide RF, Curcio CA. Anatomical correlates to the bands seen in the outer retina by optical coherence tomography: literature review and model. *Retina*. 2011;31:1609–1619.
37. Davies WI, Downes SM, Fu JK, et al. Next-generation sequencing in health-care delivery: lessons from the functional analysis of rhodopsin. *Genet Med*. 2012;14:891–899.
38. Vithana EN, Abu-Safieh L, Pelosini L, et al. Expression of PRPF31 mRNA in patients with autosomal dominant retinitis pigmentosa: a molecular clue for incomplete penetrance? *Invest Ophthalmol Vis Sci*. 2003;44:4204–4209.
39. Yuan L, Kawada M, Havlioglu N, Tang H, Wu JY. Mutations in PRPF31 inhibit pre-mRNA splicing of rhodopsin gene and cause apoptosis of retinal cells. *J Neurosci*. 2005;25:748–757.
40. Thiadens AA, Somervuo V, van den Born LI, et al. Progressive loss of cones in achromatopsia: an imaging study using spectral-domain optical coherence tomography. *Invest Ophthalmol Vis Sci*. 2010;51:5952–5957.